Electronic Supplementary Material

High-performance transparent conducting films of long single-walled carbon nanotubes synthesized from toluene alone

Er-Xiong Ding, Aqeel Hussain, Saeed Ahmad, Qiang Zhang (✉), Yongping Liao, Hua Jiang, and Esko I. Kauppinen (✉)

Department of Applied Physics, School of Science, Aalto University, Puumiehenkuja 2, 00076 Aalto, Espoo, Finland

Supporting information to https://doi.org/10.1007/s12274-019-2581-7

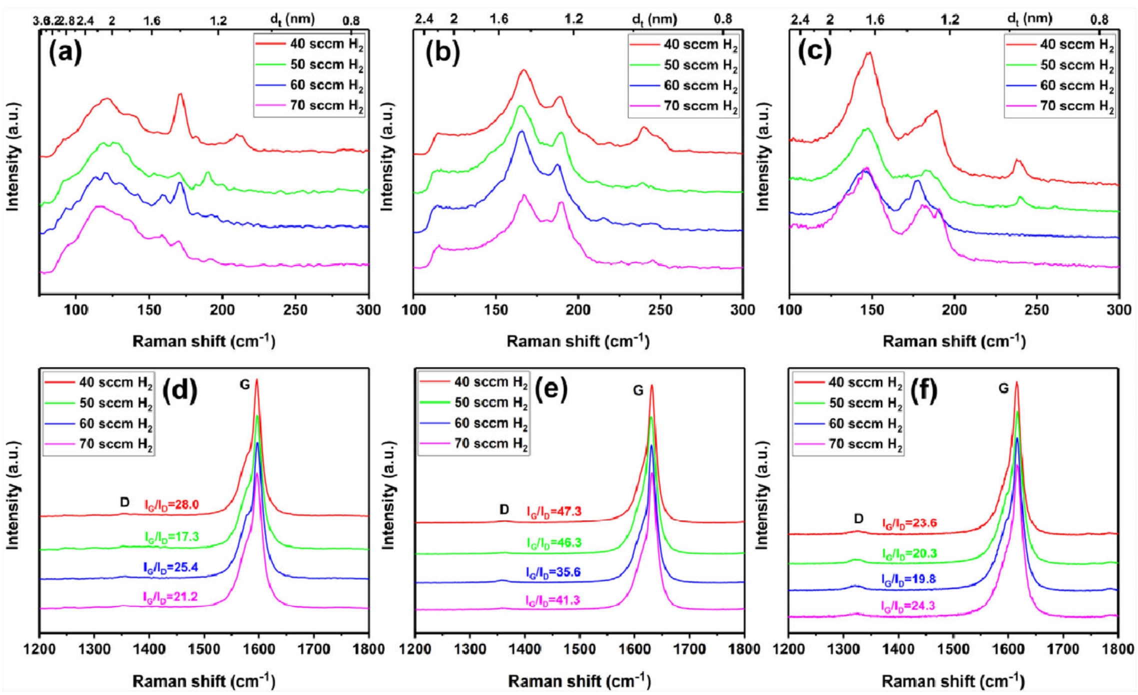

Figure S1 Raman spectra of SWCNTs synthesized at varied H_2 flow rates. (a), (b) and (c) are RBM peaks using 488 nm, 633 nm and 785 nm laser, respectively. (d), (e) and (f) are displayed to show I_G/I_D ratios of Raman spectra exited by 488 nm, 633 nm and 785 nm laser, respectively.

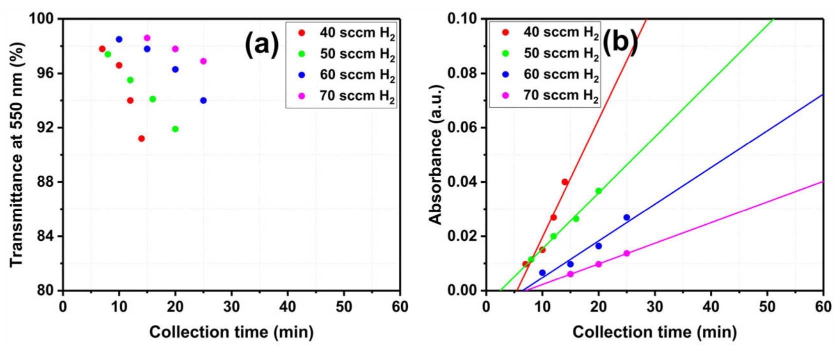

Figure S2 The relationship of deposit yield with H_2 flow rate. (a) Transmittance versus collection time. The diameter of the membrane filter is 13 mm. (b) Absorbance versus collection time. The absorbance was converted from transmittance following the Beer-Lambert law, $A = 2\text{-}\log_{10}\%T$.

Estimation of the residence time of SWCNTs in the quartz tube reactor

Only the growth zone (ca. 1000~1100 ºC) was considered for the calculation of residence time. The length of the growth zone was estimated to be ca. 0.5 m based on the temperature profile measured in our previous work [1].

Address correspondence to Qiang Zhang, qiang.zhang@aalto.fi; Esko I. Kauppinen, esko.kauppinen@aalto.fi

The flow rate of carrier gas at the growth temperature can be calculated from the flow rate at room temperature, following the ideal gas law:

$$PV = nRT \tag{1}$$

where *P*, *V* and *T* are the pressure, volume and temperature, *n* is the number of moles of gas, and *R* is the ideal gas constant. Then, the average velocity can be calculated by:

$$v = Q/A \tag{2}$$

where *v* is the average velocity, *Q* is the volumetric flow rate, *A* is the cross area of the quartz tube.

The residence time was estimated following the formula:

$$t = L/v \tag{3}$$

where *t* is the residence time, *L* is the length of the growth zone.

Thus, the residence times of the SWCNTs synthesized with carrier gas flow rates of 340 sccm, 440 sccm and 540 sccm are estimated to be ca. 7.5 s, 5.7 s, 4.6 s, respectively.

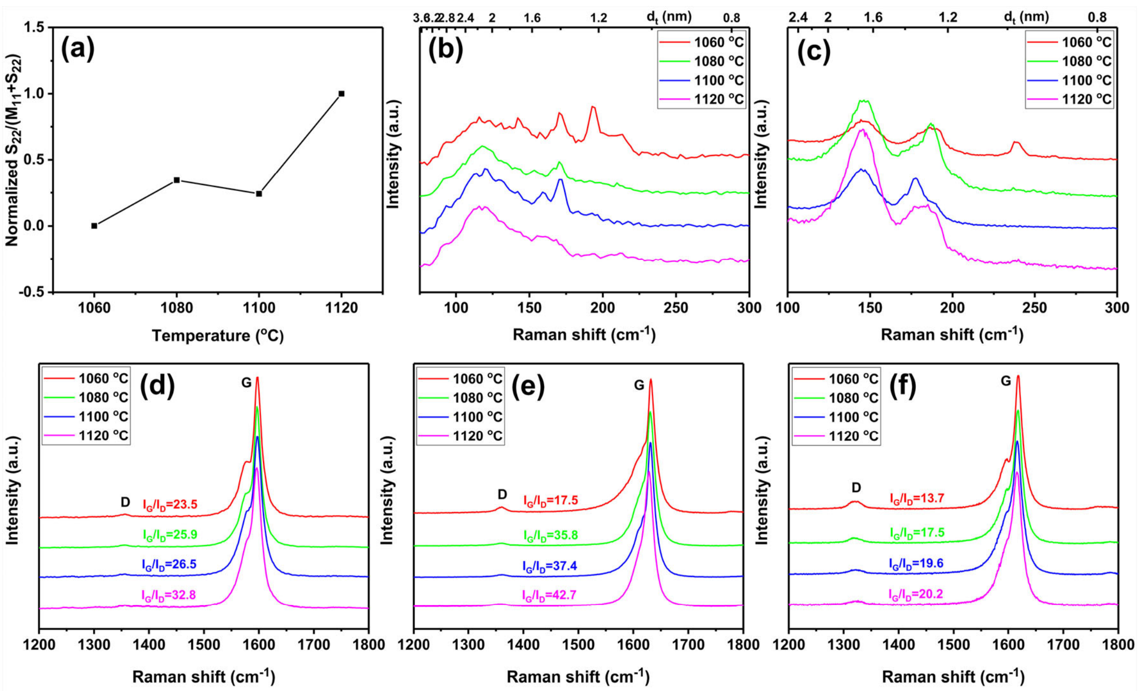

Figure S3 Temperature effect. (a) Normalized ratio of $S_{22}/(S_{22}+M_{11})$ versus temperature. (b) and (c) are RBM peaks. Laser wavelengths for (b) and (c) are 488 nm and 785 nm, respectively. (d), (e) and (f) are displayed to show I_G/I_D ratios of Raman spectra exited by 488 nm, 633 nm and 785 nm laser, respectively.

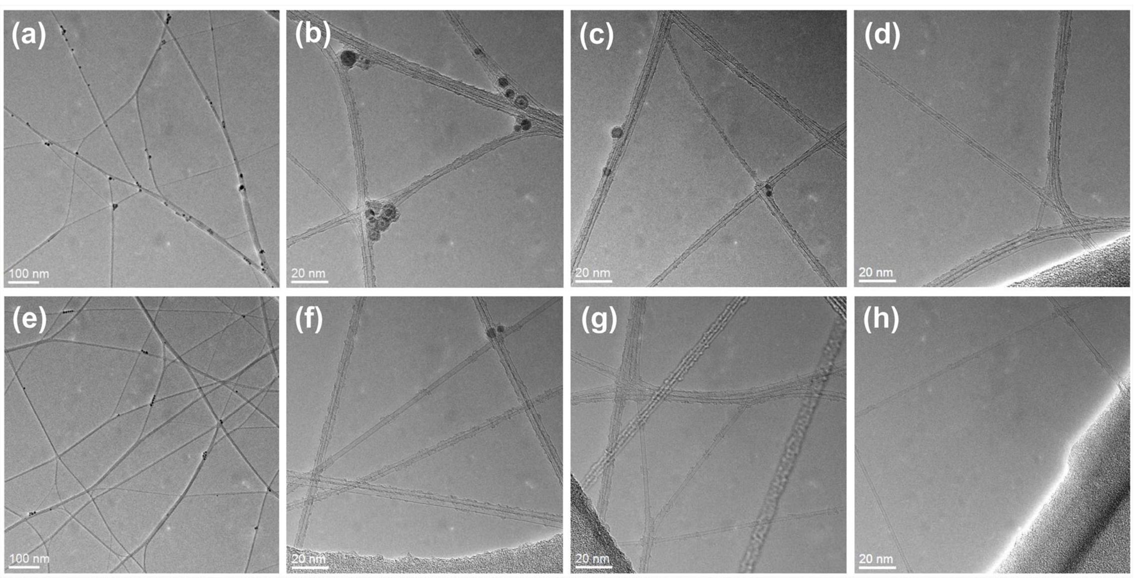

Figure S4 TEM micrographs of SWCNTs grown at different temperatures. (a)-(d) 1060 °C. (e)-(h) 1120 °C.

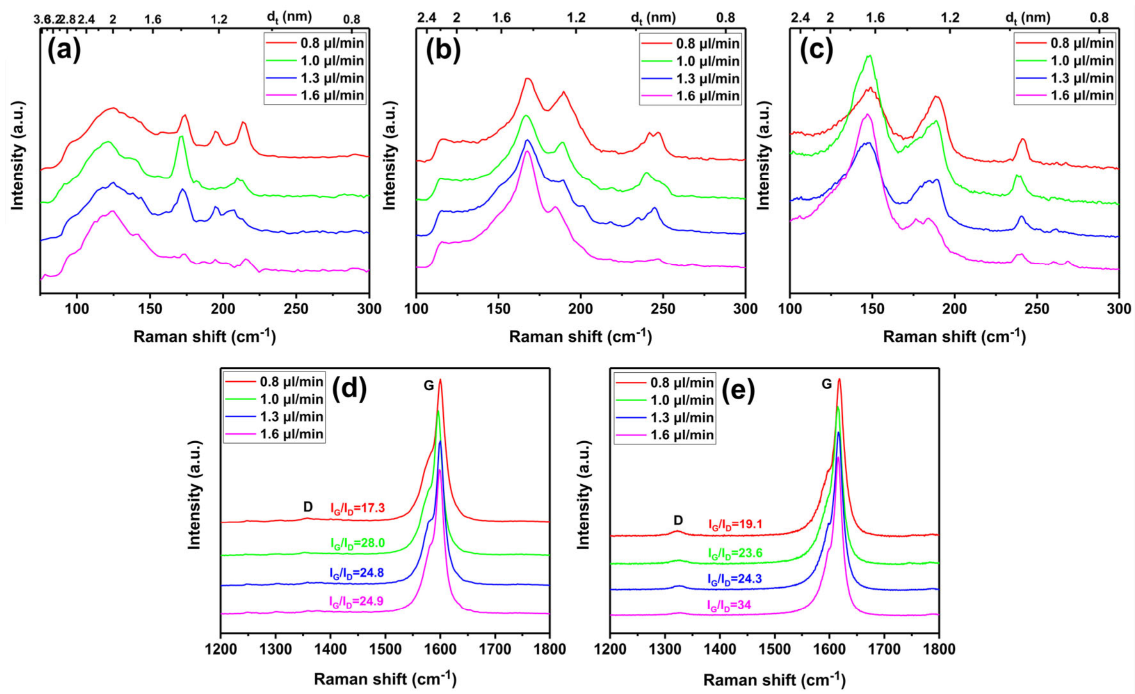

Figure S5 Raman spectra of SWCNTs collected at varied feeding rates of precursors. (a), (b) and (c) are RBM peaks exited by 488 nm, 633 nm and 785 nm laser, respectively. (d) and (e) are presented to show I_G/I_D ratios of Raman spectra exited by 488 nm and 785 nm laser, respectively.

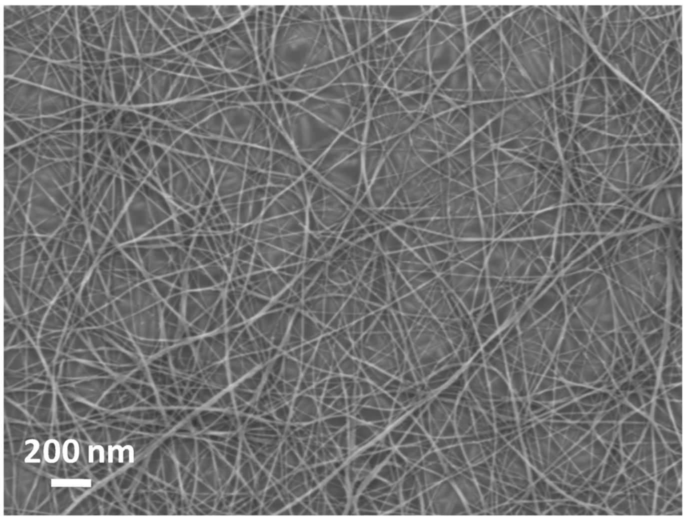

Figure S6 A typical SEM micrograph of surface morphology of a SWCNT film with a transmittance close to 90%. The film was densified by ethanol before imaging.

Table S1 Summary of the morphology features of as-synthesized SWCNTs and the optoelectronic performance of corresponding TCFs after doping treatment.

Fabrication method	D_t (nm)	L (μm)	D_{bundle} (nm)	Substrate	Dopant	R_s (ohm/sq.)	T_{550} (%)	Ref.
Dry process (micropatterning)	1.35	-	-	PEN	HNO_3	53	80	[2]
Dry process (micropatterning)	1.3	4.8	3.5	PEN	HNO_3	22	83	[3]
Dry process	1.9	7.5	7.1	Quartz	$AuCl_3$	86.8	90	[4]
Dry process	2.0	28.4	5.3	Quartz	$AuCl_3$	78	90	[5]
Dry process	1.7~2.4	20	-	PET	HNO_3	65	90	[6]
Dry process	1.1	4	1.21	Quartz	HNO_3	63	90	[7]
Dry process	1.3	13	4	Quartz	HNO_3	51	90	[8]
Dry process (doping study)	-	-	-	PET	$HAuCl_4$	40	90	[9]
Dry process	2.0	62	85% isolated	PET	HNO_3	25	90	[10]

Note: 1. D_t is the mean diameter of SWCNTs, L is the mean length of SWCNTs, D_{bundle} is the mean diameter of SWCNT bundles, R_s is the sheet resistance of SWCNT TCFs, T_{550} is the transmittance value obtained at 550 nm. 2. "–" refers to unavailable data in the reference. 3. PEN and PET stand for polyethylene naphthalate and polyethylene terephthalate, respectively. 4. The concentration of HNO_3 is 65~67 wt%, while that of $AuCl_3$ is 16 mM (acetonitrile as the solvent). The doping method can be found in the relevant reference.

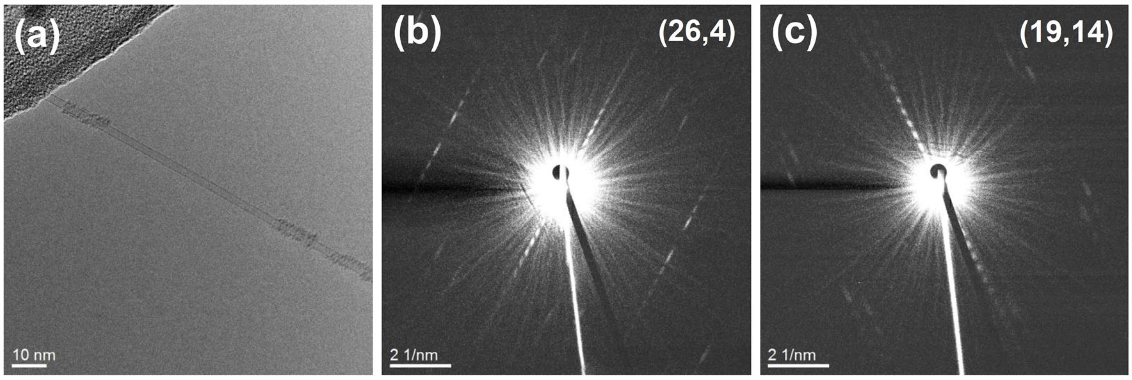

Figure S7 (a) A TEM micrograph of an individual SWCNT for the acquisition of its electron diffraction pattern. (b) and (c) are electron diffraction patterns of a near-zigzag tube (26,4) and a near-armchair tube (19,14).

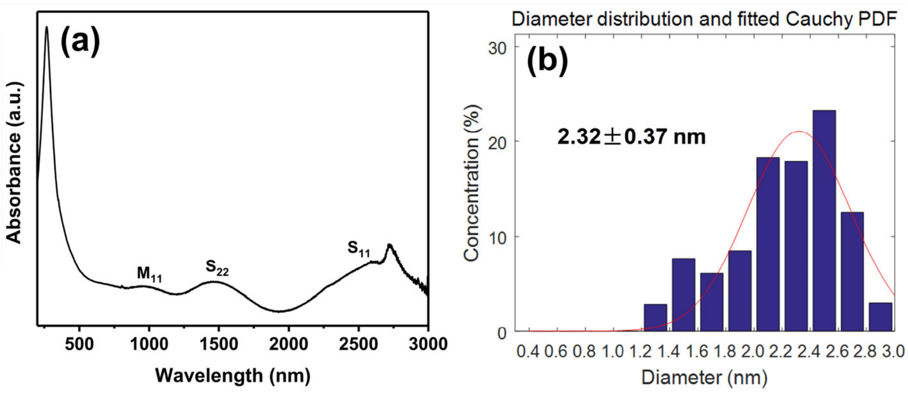

Figure S8 (a) Optical absorption spectrum of SWCNTs collected at the same conditions with those of SWCNTs for gathering electron diffraction patterns. (b) Fitted diameter distribution of SWCNTs from the absorption spectrum in (a) using a Matlab code [5].

References

[1] Ding, E.-X.; Jiang, H.; Zhang, Q.; Tian, Y.; Laiho, P.; Hussain, A.; Liao, Y.; Wei, N.; Kauppinen, E. I. Highly conductive and transparent single-walled carbon nanotube thin films from ethanol by floating catalyst chemical vapor deposition. *Nanoscale* **2017**, *9,* 17601–17609.

[2] Fukaya, N.; Kim, D. Y.; Kishimoto, S.; Noda, S.; Ohno, Y. One-step sub-10 μm patterning of carbon-nanotube thin films for transparent conductor applications. *ACS Nano* **2014**, *8*, 3285–3293.

[3] Kaskela, A.; Laiho, P.; Fukaya, N.; Mustonen, K.; Susi, T.; Jiang, H.; Houbenov, N.; Ohno, Y.; Kauppinen, E. I. Highly individual SWCNTs for high performance thin film electronics. *Carbon* **2016**, *103*, 228–234.

[4] Liao, Y.; Hussain, A.; Laiho, P.; Zhang, Q.; Tian, Y.; Wei, N.; Ding, E. X.; Khan, S. A.; Nguyen, N. N.; Ahmad, S.; et al. Tuning geometry of SWCNTs by CO_2 in floating catalyst CVD for high-performance transparent conductive films. *Adv. Mater. Interfaces* **2018**, *5,* 1801209.

[5] Ding, E.-X.; Zhang, Q.; Wei, N.; Khan, A. T.; Kauppinen, E. I. High-performance single-walled carbon nanotube transparent conducting film fabricated by using low feeding rate of ethanol solution. *R. Soc. Open Sci.* **2018**, *5,* 180392.

[6] Wang, B.-W.; Jiang, S.; Zhu, Q.-B.; Sun, Y.; Luan, J.; Hou, P.-X.; Qiu, S.; Li, Q.-W.; Liu, C.; Sun, D.-M.; et al. Continuous fabrication of meter-scale single-wall carbon nanotube films and their use in flexible and transparent integrated circuits. *Adv. Mater.* **2018**, *30*, 1802057.

[7] Mustonen, K.; Laiho, P.; Kaskela, A.; Zhu, Z.; Reynaud, O.; Houbenov, N.; Tian, Y.; Susi, T.; Jiang, H.; Nasibulin, A. G.; et al. Gas phase synthesis of non-bundled, small diameter single-walled carbon nanotubes with near-armchair chiralities. *Appl. Phys. Lett.* **2015**, *107*, 013106.

[8] Hussain, A.; Liao, Y.; Zhang, Q.; Ding, E.-X.; Laiho, P.; Ahmad, S.; Wei, N.; Tian, Y.; Jiang, H.; Kauppinen, E. I. Floating catalyst CVD synthesis of single walled carbon nanotubes from ethylene for high performance transparent electrodes. *Nanoscale* **2018**, *10*, 9752–9759.

[9] Tsapenko, A. P.; Goldt, A. E.; Shulga, E.; Popov, Z. I.; Maslakov, K. I.; Anisimov, A. S.; Sorokin, P. B.; Nasibulin, A. G. Highly conductive and transparent films of $HAuCl_4$-doped single-walled carbon nanotubes for flexible applications. *Carbon* **2018**, *130*, 448–457.

[10] Jiang, S.; Hou, P. X.; Chen, M. L.; Wang, B. W.; Sun, D. M.; Tang, D. M.; Jin, Q.; Guo, Q. X.; Zhang, D. D.; Du, J. H.; et al. Ultrahigh-performance transparent conductive films of carbon-welded isolated single-wall carbon nanotubes. *Sci. Adv.* **2018**, *4*, eaap9264.